

Propagation and organization in lattice random media

Patrick Grosfiels * and Jean Pierre Boon †

*Center for Nonlinear Phenomena and Complex Systems
Université Libre de Bruxelles, 1050 - Bruxelles, Belgium*

E. G. D. Cohen ‡

*The Rockefeller University
New York, NY 10021*

and

L.A. Bunimovich§

*School of Mathematics, Georgia Institute of Technology
Atlanta, GA 30332*

June 16, 2021

Abstract

We show that a signal can propagate in a particular direction through a model random medium regardless of the precise state of the medium. As a prototype, we consider a point particle moving on a one-dimensional lattice whose sites are occupied by scatterers with the following properties: (i) the state of each site is defined by its *spin* (up or down); (ii) the particle arriving at a site is scattered forward

*E-mail address: pgrosfi@ulb.ac.be

†E-mail address: jpboon@ulb.ac.be

‡E-mail address: egdc@rockvax.rockefeller.edu

§E-mail: bunimovh@math.gatech.edu

(backward) if the spin is up (down); (iii) the state of the site is modified by the passage of the particle, i.e. the spin of the site where a scattering has taken place, flips ($\uparrow \Leftrightarrow \downarrow$). We consider one dimensional and triangular lattices, for which we give a microscopic description of the dynamics, prove the propagation of a particle through the scatterers, and compute analytically its statistical properties. In particular we prove that, in one dimension, the average propagation velocity is $\langle c(q) \rangle = 1/(3 - 2q)$, with q the probability that a site has a spin \uparrow , and, in the triangular lattice, the average propagation velocity is independent of the scatterers distribution: $\langle c \rangle = 1/8$. In both cases, the origin of the propagation is a blocking mechanism, restricting the motion of the particle in the direction opposite to the ultimate propagation direction, and there is a specific re-organization of the spins after the passage of the particle. A detailed mathematical analysis of this phenomenon is, to the best of our knowledge, presented here for the first time.

1 Motivation

Discrete systems with simple microscopic dynamics can exhibit peculiar behavior showing some degree of complexity on a large scale. These systems have raised particular interest because they can be viewed as paradigms for complex phenomena such as growth processes, signal propagation in random media, spatio-temporal structuring in excitable media, or evolutionary dynamics [1]. In particular, phenomena such as anomalous diffusion and oscillatory propagation have been reported by Cohen and co-workers [2] who studied, numerically and theoretically, the motion of a particle in two-dimensional Lorentz Lattice Gases whose sites are occupied by scatterers which deflect the particle according to an *a priori* given rule. The most striking behavior in the particle dynamics is observed when the rule includes a feed-back of the particle on the substrate: the passage of the particle modifies the scattering property of the visited sites, e.g. if a particle arriving at a site is scattered say to the right (R), the state of the site is changed (R \Rightarrow L) such that on its next visit the particle will be scattered to the left (“flipping scatterers”). This “interaction” between the particle and the state of the scatterer modifies considerably the dynamics as compared to the classical Lorentz Lattice Gas. For instance, lattices with flipping scatterers

can yield oscillatory motion with overall propagation [2], while random fixed scatterers produce closed trajectories. Bunimovich and Troubetzkoy proved a number of theorems about the boundedness or unboundedness of the trajectories of the particle for certain lattice models, and also discussed some generalizations [3].

In order to illustrate the propagative behavior, we show in Fig.1 the case of a random Delaunay lattice [4]: here the particle arriving at a node is deflected with the largest possible angle, either to the right or to the left, depending on the state of the scatterer (which after the passage of the particle goes into the reverse state); whatever the initial configuration of the scatterers on the lattice, the particle will, after a few time steps, *always* enter a propagation phase (see the propagation *strip* shown in Fig.1).

Here we present a detailed mathematical analysis of unbounded trajectories in one-dimensional and two-dimensional (triangular) lattices. In particular we show that for *any* initial configuration of the scatterers, the particle will always propagate in a certain direction with a given average velocity. The direction of the propagation is determined by the initial velocity of the particle and the initial state of the scatterers in a small neighborhood of the initial position of the particle. On the triangular lattice the entire trajectory becomes quickly confined to a particular strip, which is bounded by two adjacent parallel lines of the lattice ¹. The propagation is due to a *blocking mechanism* which prevents the particle from moving in a direction opposite to the propagation direction for more than a few steps; thus the particle can visit any lattice site at most three times in one dimension, and six times on the triangular lattice. The blocking mechanism is due to an organization of the scatterers induced by their interaction with the moving particle, which itself is thereby forced to propagate indefinitely in a particular direction. While in one dimension the rearrangement of the scatterers after the passage of the particle is a simple mapping of the initial configuration, on the triangular lattice a self-organization of the scatterers takes place along the propagation strip: the visited sites on one of the two boundary lines are occupied by only one kind (R or L) of scatterers, while the other boundary line is occupied by only the other kind (L or R). We find another important distinction: the average propagation velocity (averaged over all possible initial distributions

¹This propagation phenomenon was first observed and analyzed on the triangular lattice by Kong and Cohen [2].

of the scatterers with a fixed ratio of R and L scatterers) in one dimension, depends on the *a priori* probability that a site has a spin \uparrow , while in the two-dimensional (triangular) lattice, it is a constant (independently of the probability that a site has a L or R scatterer).

We first consider the one dimensional lattice. In section 2, we define the 1-D system considered here, introduce the basic equations describing the microscopic dynamics, and prove propagation of the particle; section 3 is devoted to a detailed study of the statistical properties of the particle motion. The triangular lattice is treated in section 4 where particle propagation and its general and statistical properties are analyzed. All our analytical results are shown to be in agreement with our corresponding numerical simulation data obtained for one- and two-dimensional lattices. We conclude with some general comments (section 5).

2 The 1-D lattice

We consider a regular one-dimensional lattice where a single particle moves from one site to the next, with the following properties: (i) the state of each site is defined by its *spin* (up or down); (ii) the particle arriving at a site is scattered forward (backward) if the spin is up (down); (iii) the spin of the site where a scattering has taken place, flips ($\uparrow \Rightarrow \downarrow, \downarrow \Rightarrow \uparrow$)². Setting the distance between neighboring sites and the speed of the particle equal to unity, the particle moves from one lattice site to the next in one unit time step. The initial position and velocity of the particle are arbitrarily fixed, and the spins are arbitrarily distributed on the lattice with an *a priori* probability q that a site has a spin \uparrow .

2.1 Definitions

(i) Define the position $R(t)$ of the particle at time t as the location of the site r where the particle resides at time t .

²A generalization to more complicated transitions in the scattering properties of the sites has been considered for cyclic cellular automata by Bunimovich and Troubetzkoy [3] who proved a number of general theorems, without having to use explicitly the equations of motion for the particle and the equations for the dynamics of the scatterers.

(ii) Define the velocity of the particle: $C(t)$, whose value is $+1$ (when the particle moves to the right) or -1 (when it moves to the left) ³.

(iii) Define the spin (the orientation of the scatterer) ⁴ at site r , at time t , as a Boolean variable: $\eta(r, t)$, with value $+1$ (*spin up*, which does not modify the velocity of the particle), or -1 (*spin down*, which reverses the velocity of the particle from $C = +1$ to $C = -1$ or *vice versa*).

2.2 Basic equations

(1) At each time step the particle moves to a neighboring site according to its velocity, and its new position is given by the equation of motion:

$$R(t+1) = R(t) + C(t). \quad (2.1)$$

(2) The velocity of the particle at its new position is maintained or reversed, depending on the state of the spin (the orientation of the scatterer):

$$C(t+1) = C(t) \eta(R(t+1), t). \quad (2.2)$$

In $\eta(R(t+1), t)$, t refers to the time corresponding to the state of the spin *before* flipping; we shall denote by $t+$ the time just *after* the particle arrived at a site and made its spin flip ($\uparrow \Leftrightarrow \downarrow$).

(3) The spin of the site hit by the particle is reversed (all other spins remain unchanged):

$$\begin{aligned} \eta(r, t+1) &= \eta(r, t) (1 - \delta_{r, R(t+1)}) - \eta(r, t) \delta_{r, R(t+1)} \\ &= \eta(r, t) (1 - 2 \delta_{r, R(t+1)}); \end{aligned} \quad (2.3)$$

so

$$\eta(R(t+1), t+1) = -\eta(R(t+1), t). \quad (2.4)$$

Equations (2.1), (2.2), and (2.4) are the basic equations of the dynamics on the 1-D lattice.

³With the convention that the positive direction on the 1-D lattice is from left to right, we can omit vectorial notation for simplicity.

⁴In previous publications [2] the scatterers were indicated as to their right or left scattering properties (R or L); for the 1-D case a representation of the scatterers by up or down spins is more convenient.

2.3 Propagative motion

We say that the particle propagates in one direction on the one-dimensional lattice, if it visits any lattice site not more than some fixed finite number of times. This definition implies that the trajectory of the particle tends to $+\infty$ or $-\infty$, when the time goes to infinity. Indeed since the particle cannot return to a site after it has visited it a finite number of times, the particle must remain on a semi-line to the right (or to the left) of this site, which holds equally for the next visited site. Consequently the position of the particle must approach $+\infty$ or $-\infty$ when $t \rightarrow \infty$.

We now formulate the propagation theorem.

Theorem 1 : A particle moving from site to site in a one-dimensional lattice fully occupied with flipping scatterers (spins), propagates in one direction, independently of the initial distribution of the spins on the lattice. The propagation direction depends upon the orientation of the spin at the origin of the particle motion ($r = 0$) and of that at the site $r = +1$, if the initial particle velocity $C(t = 0+) \equiv C(0+) = +1$, or alternatively of that at site $r = -1$, if $C(0+) = -1$.

Proof : Without loss of generality we assume that the initial velocity of the particle is positive, i.e., $C(0+) = 1$. Then we have to consider two cases according to whether the spin of the site at the origin ($r = 0, t = 0$) is either \uparrow or \downarrow (see Fig.2 for illustration of the proof).

A. If at $t = 0+$, $\eta(R(0), 0+) = \eta(0, 0+) = -1$, there are two possibilities: (1) the spin at time 0 at the position $R(1)$ is \uparrow , i.e. $\eta(R(1), 0) = \eta(1, 0) = 1$. Then at time $1+$, $C(1+) = 1$ and $\eta(R(1), 1+) = \eta(1, 1+) = -1$; (2) the spin at time 0 at the position $R(1)$ is \downarrow , i.e., $\eta(R(1), 0) = \eta(1, 0) = -1$. At time $1+$, $C(1+) = -1$ and $\eta(1, 1+) = +1$, while at time $2+$, $C(2+) = +1$ and $\eta(R(2), 2+) = \eta(0, 2+) = 1$. Then at time $3+$, $C(3+) = 1$ and $\eta(R(3), 3+) = \eta(1, 3+) = -1$.

Therefore in both cases (1) and (2), the system is in a state where the particle is at $r = 1$, leaving the visited sites with the velocity $+1$ ($C(1+) = 1$ in case (1) and $C(3+) = 1$ in case (2)), while the scatterer at this site ($r = 1$) is \downarrow . Thus we retrieve the initial situation shifted by one lattice unit to the right, and consequently the same analysis can be repeated for the next site, and so on.

We call the state of the system when $C(t+) = 1$ and $\eta(R(t), t+) = -1$, a left *blocking pattern*. So the above analysis shows that a left blocking pattern at the site $R(t)$ will be shifted to a left blocking pattern at the next site to the right of $R(t)$ at $R(t)+1$, in one time step in case (1) ($R(t+1) = R(t)+1$), or in 3 time steps in case (2) ($R(t+3) = R(t)+1$), leading, in both cases, to propagation of the particle to the right.

B. If at $t = 0+$, $\eta(R(0), 0+) = \eta(0, 0+) = +1$, there are again two possibilities:

(1) the spin at time 0 at the position $R(1)$ is \uparrow , i.e. $\eta(R(1), 0) = \eta(1, 0) = +1$. Then $C(1+) = 1$ and $\eta(R(1), 1+) = \eta(1, 1+) = -1$, and the same blocking pattern obtains at $r = 1$ at the time $t = 1+$, as in case A(1).

(2) the spin at time 0 at the position $R(1)$ is \downarrow , i.e. $\eta(1, 0) = -1$. Therefore $C(1+) = -1$ and $\eta(R(1), 1+) = \eta(1, 1+) = 1$. Then at time $2+$, $C(2+) = -1$ and $\eta(R(2), 2+) = \eta(0, 2+) = -1$, and we obtain a situation opposite to that in Case A(2), which implies that there is now a *right* blocking pattern leading to a propagation to the left. Thus the same analysis is applicable here, if one changes positive velocities and position changes to negative ones and vice-versa.

We conclude (see Fig.2) that there are three cases where the initial conditions for C and η produce a left blocking mechanism and a propagation to the right:

$$\begin{aligned} \text{A(1): } & C(0+) = +1, \eta(0, 0+) = -1, \eta(1, 0) = +1, \\ \text{A(2): } & C(0+) = +1, \eta(0, 0+) = -1, \eta(1, 0) = -1, \\ \text{B(1): } & C(0+) = +1, \eta(0, 0+) = +1, \eta(1, 0) = +1, \end{aligned}$$

and one initial condition:

$$\text{B(2): } C(0+) = +1, \eta(0, 0+) = +1, \eta(1, 0) = -1,$$

which produces a right blocking mechanism and a propagation to the left .

Clearly the same analysis holds if the initial velocity of the particle is to the left: for $C(0+) = -1$, there are three cases where the propagation is to the left, and one where the propagation is to the right. Propagation in the direction of the initial velocity occurs in three out of four cases. Notice that by *fixing* the initial condition with only *one* spin: $\eta(R(0), 0+) = -1$, i.e. the spin is set \downarrow at the origin, the particle always propagates in the direction of its initial velocity.

Two corollaries follow from *Theorem 1*.

Corollary 1 : A particle moving on a 1-D lattice fully occupied with flipping scatterers visits any lattice site at most three times.

The proof follows immediately from *Theorem 1* as a consequence of the blocking mechanism.

Corollary 2 : The propagation velocity C_ℓ between two sites separated by a distance ℓ containing u spins \uparrow , is $C_\ell = (3 - 2u/\ell)^{-1}$.

Proof : We first note that the time t_ℓ taken by the particle to cover the distance ℓ equals ℓ plus twice the number of times the particle visits a site with spin \downarrow , forcing the particle into a backward-forward motion. Thus $t_\ell = \ell + 2(\ell - u) = 3\ell - 2u$. Since $C_\ell = \ell/t_\ell$, the corollary follows immediately.

Finally we note that after the passage of the particle through the lattice, all spins of the visited sites have been reversed ($\uparrow \Leftrightarrow \downarrow$) with a shift of one lattice site opposite to the ultimate velocity of propagation. This reorganization of the spins, which is a consequence of the blocking mechanism, is illustrated in Fig.3.

3 Statistical properties

Statistical properties are obtained by considering average quantities $\langle \dots \rangle$, where the average is taken over all initial spin configurations, with the initial *a priori* probability q that a site is in the state \uparrow .

3.1 Average velocity

From *Corollary 2*, it follows immediately that the average time $\langle t_\ell \rangle$ taken by the particle to cover a finite segment of length ℓ on the 1-D lattice is: $\langle t_\ell \rangle = 3\ell - 2\langle u \rangle = \ell(3 - 2q)$. Then the average propagation velocity $\langle c(q) \rangle \equiv c(q)$ is given by

$$c(q) = \ell / \langle t_\ell \rangle = 1 / (3 - 2q), \quad (3.1)$$

independently of the direction of propagation and regardless of the way the spins are organized. Examples are shown in Fig.4.

3.2 Time evolution

The equation of motion of the particle can be written in terms of two Boolean variables:

- (i) the occupation variable $n(r, t)$, which is equal to 1 if the particle is at site r at time t *for the first time*; otherwise $n(r, t) = 0$;
- (ii) the state of the spin at site r at time t : $\xi_{\uparrow}(r, t) = 1$ if the spin is \uparrow , and $\xi_{\downarrow}(r, t) = 1$ if the spin is \downarrow , with $\sum_{j=\uparrow,\downarrow} \xi_j = 1$.⁵ Then the equation for $n(r, t)$ reads

$$n(r, t) = \xi_{\uparrow}(r-1, 0) n(r-1, t-1) + \xi_{\downarrow}(r-1, 0) n(r-1, t-3), \quad (3.2)$$

which is a microscopic equation.

We now define $P_1(r, t) = \langle n(r, t) \rangle$, the probability that the particle, starting at the origin, visits site r at time t *for the first time*. In the following we shall use $f(r, t) \equiv P_1(r, t)$ for short, with the property $\sum_t P_1(r, t) \equiv \sum_t f(r, t) = 1, \forall r > 0$, which follows from the fact that each site will have a first visit. We also have $\langle \xi_{\uparrow}(r, 0) \rangle = q$ and $\langle \xi_{\downarrow}(r, 0) \rangle = 1 - q, \forall r$. Averaging the basic equation (3.2) over all initial configurations and using the fact that $\langle \xi n \rangle$ on the r.h.s. of (3.2) can be written as $\langle \xi \rangle \langle n \rangle$ then yields

$$f(r+1, t+1) = q f(r, t) + (1-q) f(r, t-2), \quad (3.3)$$

which shows a formal analogy with the equation for the biased random walk (BRW)⁶. For convenience in the forthcoming development, we perform a shift of variable ($t \rightarrow t+3$) to rewrite Eq.(3.3) as

$$f(r+1, t+3) = q f(r, t+2) + (1-q) f(r, t). \quad (3.4)$$

Considering that the particle, arriving from the left, is at $r=0$ for the first time at $t=0$ with unknown velocity, and that the spin at $r=-1$ is down, the initial conditions are given by

$$f(r, t=0) = \delta_{r,0}; \quad f(r, t=1) = q \delta_{r,+1}; \quad f(r, t=2) = q^2 \delta_{r,+2}. \quad (3.5)$$

⁵Notice the difference between $\eta = \pm 1$ in section 2.2 [5] and $\xi_j = \{0, 1\}$, which is the quantity used in practice for numerical simulations.

⁶The BRW equation [6] reads $g(r+1, t+1) = h g(r, t) + (1-h) g(r+2, t)$, $h \neq 0, 1$, where $g(r, t)$ is the distribution of the random walker which, at each time step, moves to the right or to the left with probability h and $1-h$ respectively (for $h = 1/2$, the equation describes the usual random walk). For a comparison with Eq.(3.3), see also [7].

Introducing the space-Fourier transform $f_k(t) = \mathcal{F}\{f(r, t)\}$ and its discrete Laplace transform $\tilde{f}_k(s) = \mathcal{L}\{f_k(t)\}$, we note that

$$\begin{aligned} \mathcal{L}\mathcal{F}\{f(r+n, t+m)\} &= e^{ikn}[e^{ms}\tilde{f}_k(s) - e^{ms}f_k(0) - e^{(m-1)s}f_k(1) - \\ &\quad \dots - e^s f_k(m-1)]. \end{aligned} \quad (3.6)$$

Equation (3.4) is then Fourier-Laplace transformed to yield

$$\begin{aligned} e^{ik}e^s [e^s[e^s(\tilde{f}_k(s) - f_k(0)) - f_k(1)] - f_k(2)] &= \\ q e^s[e^s(\tilde{f}_k(s) - f_k(0)) - f_k(1)] + (1-q)\tilde{f}_k(s), \end{aligned} \quad (3.7)$$

with

$$f_k(0) = 1; \quad f_k(1) = q e^{ik}; \quad f_k(2) = q^2 e^{2ik}, \quad (3.8)$$

which follow from the initial conditions (3.5). Setting $z = e^s$ and $\kappa = e^{ik}$, the solution to Eq.(3.6) reads

$$\tilde{f}_\kappa(z) = z \frac{z^2 + q(\kappa - 1/\kappa) + q^2(\kappa^2 - 1)}{z^2(z - q/\kappa) - (1 - q)/\kappa}. \quad (3.9)$$

The function $\tilde{f}_\kappa(z)$ can be explicitly inverted in time and space for $q = 1$ and $q = 0$; the results for $f(r, t) \equiv P_1(r, t)$ are given, as expected, in terms of δ -functions, $\delta(r, t)$ for $q = 1$ and $\delta(r, t/3)$ for $q = 0$. When $q \neq 0$ or 1 , we consider the case $\kappa = 1$, i.e. the limit of long wavelengths ($k = 0$), for which the poles of the above transform can be computed easily⁷; we obtain

$$\tilde{f}_{\kappa=1}(z) = z^3 [(z - z_0)(z - z_+)(z - z_-)]^{-1}, \quad (3.10)$$

where

$$z_0 = 1; \quad z_\pm = (1 - q)^{1/2}(\cos \varpi \mp i \sin \varpi), \quad (3.11)$$

with

$$\cos \varpi = -\frac{1}{2}(1 - q)^{1/2}, \quad \sin \varpi = \frac{1}{2}(3 + q)^{1/2}. \quad (3.12)$$

⁷The computation for $\kappa \neq 1$ (with $q \neq 0$ or 1) is quite involved and the explicit analytical results are not very instructive.

The function $\tilde{f}_{\kappa=1}(z)$ is then inverted (using residues) to obtain the explicit expression for $f_{k=0}(t) = \sum_r f(r, t)$; after some straightforward algebra, we find

$$f_{k=0}(t) = \frac{1}{3-2q} [1 + 2(1-q) e^{-\zeta t} (\cos \varpi t + \varphi \sin \varpi t)], \quad (3.13)$$

with

$$\zeta = \frac{1}{2} \log \frac{1}{1-q}, \quad \varpi = \arctan -\sqrt{\frac{3+q}{1-q}}, \quad \varphi = \frac{q}{(1-q)^{1/2}(3+q)^{1/2}}. \quad (3.14)$$

The case $q = 0$ provides a trivial but illustrative example ; it is straightforwardly verified that the solution then reads

$$f_{k=0}^{q=0}(t) = \frac{1}{3} (1 + 2 \cos \frac{2\pi}{3} t), \quad (3.15)$$

which is a repeated sequence of values $(1, 0, 0)$ as can be inferred from the dynamics of the particle when all spins are initially down. The case $q = 1$ (all spins initially up) yields the obvious result $f_{k=0}^{q=1}(t) = 1$.

The long-time behavior of $f_{k=0}(t)$ is easily obtained from the limit $s \rightarrow 0$ of $\tilde{f}_{k=0}(s)$ by expanding $\tilde{f}_{k=0}(s)$ to lowest order in s

$$\lim_{s \rightarrow 0} \tilde{f}_{k=0}(s) = \frac{1}{s} \frac{1}{3-2q}, \quad (3.16)$$

which yields by Laplace inversion

$$\lim_{t \rightarrow \infty} f_{k=0}(t) = \frac{1}{3-2q}. \quad (3.17)$$

This result, combined with (3.1), shows that

$$\lim_{t \rightarrow \infty} \sum_r P_1(r, t) = c(q). \quad (3.18)$$

In Fig.5 we show that the above analytical results and the simulation data are in perfect agreement. An alternative derivation of (3.18), directly based on the analysis of the particle dynamics, is given in Appendix A.

3.3 Space evolution

We now construct an explicit analytical expression in r and t for the probability that the particle visits, for the first time, site r at time t , i.e. the function $P_1(r, t)$. Consider, on the 1-D lattice, a segment with length ℓ (in lattice units) and with spin configuration $\{\eta_i\} = (\eta_0, \eta_1, \dots, \eta_\ell)$, where $\eta_i = \uparrow$ or \downarrow . Suppose that at time zero, the particle is at site $r = 0$ with velocity $C(0+) = +1$, and the spin is $\eta_0 = \downarrow$. Then the time τ taken by the particle to travel the distance ℓ is $\tau(\ell, \{\eta_i\}) = 1 + N_\uparrow + 3N_\downarrow$, where N_\uparrow and N_\downarrow are the numbers of sites with spin up and spin down, respectively, between $r = 1$ to $r = \ell - 1$ (since the spin η_ℓ is unimportant). So $N_\downarrow = \ell - 1 - N_\uparrow$ and

$$\tau(\ell, \{\eta\}) = 3\ell - 2(1 + N_\uparrow). \quad (3.19)$$

The probability for the particle to be for the first time at site r at time t for a given spin configuration is

$$P_1(r, t; \{\eta_i\}) = \delta_{t, \tau(r, \{\eta_i\})}, \quad (3.20)$$

so that

$$P_1(r, t) = \sum_{\{\eta_i\}} \delta_{t, \tau(r, \{\eta_i\})} P(\{\eta_i\}), \quad (3.21)$$

where $P(\{\eta_i\})$ is the probability of the spin configuration $\{\eta_i\}$

$$P(\{\eta_i\}) = \binom{r-1}{N_\uparrow} q^{N_\uparrow} (1-q)^{r-1-N_\uparrow}, \quad (3.22)$$

with q the probability that a site has spin \uparrow . Furthermore, using (3.19) for $\ell = r$, we have

$$\begin{aligned} P_1(r, t) &= \sum_{N_\uparrow=0}^{r-1} \delta_{t, 3r-2(1+N_\uparrow)} \binom{r-1}{N_\uparrow} q^{N_\uparrow} (1-q)^{r-1-N_\uparrow} \\ &= \binom{r-1}{\frac{1}{2}(3r-t-2)} q^{\frac{1}{2}(3r-t-2)} (1-q)^{\frac{1}{2}(t-r)} \\ &= \binom{r-1}{\frac{1}{2}(t-r)} q^{(r-1)-\frac{1}{2}(t-r)} (1-q)^{\frac{1}{2}(t-r)}, \end{aligned} \quad (3.23)$$

and it is a matter of simple algebra to show that (3.23) is a solution of the difference equation (3.3). This solution is valid for any spin configuration with $N_{\uparrow} = 0, \dots, r - 1$. For the trivial cases where all spins are either up or down, one can easily verify the obvious results

$$P_1^{N_{\uparrow}=r-1}(r, t = r) = 1 ; \quad P_1^{N_{\uparrow}=0}(r, t = 3r - 2) = 1 . \quad (3.24)$$

An example of space-time evolution of the system based on Eq.(3.23) is shown in Fig.6.

3.4 Long-time large-distance behavior

An interesting result follows from the computation of the average time the particle takes to cover a distance r when r is large. In (3.23), we set $(1-q) = p$ and $(t - r) = 2a$, and we consider r large (i.e. $r \gg 1$); then $P_1(r, t)$ can be rewritten as

$$P_1(r, a) = \binom{r}{a} p^a q^{r-a} . \quad (3.25)$$

Using a standard procedure of probability theory [8], we have

$$\langle a \rangle = \left[\sum_a a \binom{r}{a} p^a q^{r-a} \right]_{q=1-p} = \left[p \frac{\partial}{\partial p} (p+q)^r \right]_{q=1-p} = r p , \quad (3.26)$$

which we rewrite as

$$\frac{1}{2}(\langle t \rangle - r) = r(1 - q) , \quad \text{or} \quad \frac{\langle t \rangle}{r} = 3 - 2q , \quad (3.27)$$

i.e., we retrieve the expression for the average velocity $c(q) = (3 - 2q)^{-1}$.

We now compute the explicit analytical expression of $P_1(r, t)$ for large r . We consider p, q fixed, and $r \gg 1$, such that $\frac{1}{r}|a - rp| \rightarrow 0$, which is equivalent to $[\frac{t}{r} - (3 - 2q)] \rightarrow 0$, the limit we expect for long times. Then using Stirling's formula in the binomial coefficient of (3.25), and performing a Taylor expansion in $\delta a = a - rp$, [9] we obtain

$$P_1(r, a)|_{r \gg 1} = (2\pi r p q)^{-1/2} \exp(-\delta a^2 / 2r p q) . \quad (3.28)$$

Noting that $\delta a/r = \frac{1}{2}[(t/r) - (3 - 2q)]$, (3.28) can be rewritten as

$$P_1(r, t)|_{r \gg 1} = \frac{1}{\sqrt{2\pi}(rpq)^{1/2}} \exp -\frac{(r - \langle r(t) \rangle)^2}{2\gamma r}, \quad (3.29)$$

with

$$\langle r(t) \rangle = t(3 - 2q)^{-1} = c(q)t, \quad \text{and} \quad \gamma = 4pq(3 - 2q)^{-2} = 4pqc^2(q). \quad (3.30)$$

In Fig.7 we show a comparison between simulation data, the computation of the binomial expression (3.23), and the analytical result (3.29).

The connection with the results of subsection 3.2, in particular with the function $f_{k=0}(t \rightarrow \infty)$, is easily established by taking the Fourier transform of (3.29) in the limit $k = 0$, that is $\int_0^\infty dr P_1(r, t)$; by setting $r = x^2$, $\alpha = (3 - 2q)/\sqrt{8pq}$, and $\beta = \alpha \langle r \rangle$, we obtain from (3.29)

$$\frac{1}{2} \int_0^\infty dx P_1(x) = \frac{1}{2\sqrt{2\pi}(pq)^{1/2}} e^{2\alpha\beta} \int_0^\infty dx e^{-\alpha^2 x^2 - \beta^2/x^2} = \frac{1}{3 - 2q}, \quad (3.31)$$

which is exactly the result (3.17).⁸

3.5 Total probability distribution

In section 2.3 we showed that any lattice site can be visited at most three times (*Corollary 1*). So we define $P_1(r, t)$, $P_2(r, t)$, and $P_3(r, t)$, as the probabilities that the particle be at site r at time t for the first, second, and third time, respectively. We also introduce the probability $P_{21}(r, t)$ for the particle to be at site r at time t for the second time, without ever having visited the next site (at $r + 1$); then the particle must have visited site r two time-steps earlier and this was a first-time visit and the spin was down (see Fig.8a). Therefore

$$P_{21}(r, t) = (1 - q)P_1(r, t - 2). \quad (3.32)$$

Equation (3.3) for $f(r, t) = P_1(r, t)$ is regained by noticing that a first visit at site $r + 1$ at time $t + 1$ results from either a direct displacement of the particle

⁸Note that the factor 1/2 on the l.h.s. of (3.31) comes from the fact that the binomial coefficient in (3.25) must be interpreted as zero if r and a are not of the same parity since r and t must have same parity.

from r to $r + 1$ when the spin at r is up, i.e. $qP_1(r, t)$, or a second visit at r two time-steps earlier, as described above; so the equation for $P_1(r, t)$ reads

$$\begin{aligned} P_1(r + 1, t + 1) &= qP_1(r, t) + P_{21}(r, t) \\ &= qP_1(r, t) + (1 - q)P_1(r, t - 2), \end{aligned} \quad (3.33)$$

which is exactly Eq.(3.3), with $f(r, t) \equiv P_1(r, t)$.

Now to obtain an expression for $P_2(r, t)$, two cases must be considered: the first is that of Fig.8a, which yields the contribution given by (3.32), and the second, illustrated in Fig.8b, contributes $q(1 - q)P_1(r, t - 2)$. Consequently

$$P_2(r, t) = (1 - q^2)P_1(r, t - 2). \quad (3.34)$$

There is only one situation which produces three consecutive visits to the same site, as shown in Fig.8c: the site must have been visited for the first time four time-steps earlier, and the particle must have moved twice backwards during these four time-steps, which yields

$$P_3(r, t) = (1 - q)^2 P_1(r, t - 4). \quad (3.35)$$

So the *total* probability that the particle be at site r at time t reads

$$P(r, t) = P_1(r, t) + (1 - q^2)P_1(r, t - 2) + (1 - q)^2 P_1(r, t - 4), \quad (3.36)$$

with the property $\sum_r P(r, t) = 1, \forall t$.

The long-time behavior of the total probability $P(r, t)$ is readily obtained by taking $t \gg 1$ in (3.36), which yields

$$P(r, t)|_{t \gg 1} = (3 - 2q) P_1(r, t)|_{t \gg 1}. \quad (3.37)$$

Since $t \gg 1$ also implies $r \gg 1$, it follows from (3.29) that

$$P(r, t)|_{t \gg 1} = \sqrt{\frac{2}{\pi}} \frac{1}{(\gamma r)^{1/2}} \exp -\frac{(r - \langle r(t) \rangle)^2}{2\gamma r}. \quad (3.38)$$

where $\gamma = 4c^2 pq$, $\langle r(t) \rangle = c(q)t$ (see (3.30)). Alternatively we write (3.38) as

$$P(r, t)|_{t \gg 1} = \sqrt{\frac{2}{\pi}} \frac{3 - 2q}{2(pqr)^{1/2}} \exp -\frac{(t - \langle t \rangle)^2}{2(4pq)r}, \quad (3.39)$$

with $\langle t \rangle = r/c(q)$. Then the following properties, obtained from (3.38) and (3.39),

$$P(r = \langle r(t) \rangle, t \rightarrow \infty) = \frac{1}{\sqrt{2\pi}} \left(\frac{(3-2q)^3}{q(1-q)} \right)^{1/2} \frac{1}{t^{1/2}}, \quad (3.40)$$

and

$$\langle (t - \langle t \rangle)^2 \rangle^{1/2} = 2\sqrt{2pq} r^{1/2} \quad (3.41)$$

show that, for long times, the amplitude of the probability distribution $P(r, t)$ decays like $t^{-1/2}$ and its width grows like \sqrt{r} .

We also note that, by taking the sum over r in (3.36), followed by the long-time limit ($t \gg 1$), we obtain

$$1 = (3-2q) \lim_{t \rightarrow \infty} \sum_r P_1(r, t), \quad \text{or} \quad \lim_{t \rightarrow \infty} \sum_r P_1(r, t) = c(q), \quad (3.42)$$

in accordance with our previous results (see subsection 3.2). In Fig.7 we show the long-time behavior of $P_1(r, t)$, which is the same (within a constant factor, see (3.37)) as that of $P(r, t)$.

Finally it is interesting to note that $P(r, t)$, as given by (3.39), is the solution of the differential equation

$$\partial_r P(r, t) + \frac{1}{c} \partial_t P(r, t) = \frac{1}{2} (4pq) \partial_t^2 P(r, t), \quad (3.43)$$

which can be shown to be the continuous limit of the difference equation for $P(r, t)$ [7]. The appearance of a Gaussian distribution in time, (3.39), and the differential equation with propagation (3.43) for long times are natural consequences of the averaging over the initial spin distributions.

4 The 2-D triangular lattice

We consider the motion of a particle on a triangular lattice fully occupied by *rotators* (flipping scatterers) which rotate the velocity vector of the particle by an angle of $2\pi/3$ either to the right or to the left, depending on whether

the rotator on the site hit by the particle is a R or a L scatterer, respectively.⁹ The state of the rotator at the site where the scattering took place, changes: $R \Leftrightarrow L$. Simulations show that, whatever the initial configuration of scatterers, the particle always goes into a propagation phase in the direction of one of the lattice axes [2]. An example is given in Fig.9. Here we show how propagation can be proved mathematically, and we derive the statistical properties of the dynamics of the particle.

4.1 Definitions

(i) The propagation of the particle on the triangular lattice always takes place in a *strip* which is defined as follows: a strip is a region of the triangular lattice bounded by two adjacent (parallel) lines, both oriented along one of the lattice axes.

(ii) In accordance with the 1-D case, we define particle propagation as follows: a particle propagates in one direction in a strip if its motion is confined to the strip (defined by its initial velocity and its velocity after the first scattering event) where the particle visits any site not more than a fixed number of times.

(iii) The particle's velocity vector at time t is denoted by $\mathbf{C}(t)$.

4.2 The propagation theorem

Theorem 2: For any initial distribution of scatterers on a triangular lattice, a moving particle propagates in one particular direction through a strip on the lattice; this strip and the direction of propagation along it depend on the initial configuration of the scatterers at the origin (the initial position of the particle) and at three neighboring sites; these four sites form a parallelogram whose orientation determines the propagation strip.

Proof: First we show that for each possible initial scatterers configuration, a propagation of the particle will occur in one of four strips, as sketched in Fig.10 (propagation directions and strips are indicated by F(forwards), U(upwards), D₁ and D₂(downwards)). The strip in which the particle will

⁹Although the spin notation is applicable to the rotators (with $R \equiv \uparrow$ and $L \equiv \downarrow$), the right (R) and left (L) characterization of the scatterers, as used in [2], is more convenient for our discussion of the triangular lattice.

propagate (F, U, D₁ or D₂) depends on the initial velocity direction $\mathbf{C}(t_0)$, and on the initial state (R or L) of the four sites forming a parallelogram which contains $\mathbf{C}(t_0)$. There are four such parallelograms, hence four possible directions (see Fig.10):

$$\textcircled{1}\textcircled{2}\textcircled{3}\textcircled{6} \rightarrow \text{F}, \textcircled{1}\textcircled{2}\textcircled{4}\textcircled{7} \rightarrow \text{U}, \textcircled{1}\textcircled{2}\textcircled{3}\textcircled{8} \rightarrow \text{D}_1, \textcircled{1}\textcircled{2}\textcircled{4}\textcircled{5} \rightarrow \text{D}_2.$$

Then we demonstrate that once the particle is inside a strip (at one of the sites indicated by $\textcircled{*}$ in Fig.10), it never leaves this strip. Like in 1-D, the key ingredient of the ultimate unidirectional propagation of a particle on a triangular lattice fully occupied with flipping (R and L) scatterers, is the existence of a blocking mechanism. On the triangular lattice, this mechanism produces a *blocking pattern* based on a *zig-zag* path of length four (in lattice unit lengths), which contains parallel velocity vectors at even or at odd times (see examples in Fig.11), and which prohibits particle motion more than one lattice unit length in the direction opposite to the propagation direction; as a consequence any site visited by the particle cannot be visited more than six times (see *Corollary 2* below). The result is that the particle propagates in a strip in the direction naturally defined by the blocking pattern.

Assume that a blocking pattern has been formed at the sites visited by the particle at times $t, t + 1, t + 2$ and $t + 3$, so that the vectors $\mathbf{C}(t+)$ and $\mathbf{C}((t + 2)+)$, and $\mathbf{C}((t + 1)+)$ and $\mathbf{C}((t + 3)+)$ are parallel, respectively (see Fig.11a). Then such a zig-zag trajectory can continue in two ways: either the particle continues directly its zig-zag motion at the next time step (see Fig.12a), or it turns back (Fig.12b). Obviously, the direct continuation of the zig-zag trajectory leads to propagative motion. So in order to prove propagation, we only have to consider the result of the turn back motion, and show that the particle nevertheless continues to move along the strip defined by the zig-zag direction along which it was moving from time t to time $t + 3$. Now when the particle turns back, its trajectory creates a triangle (Fig.12b) where from a zig-zag path emerges (Fig.12c). Propagation then occurs as a consequence of the fact that backward motion at time $t + 4$, necessarily produces a blocking pattern, which forbids the particle to move more than one lattice unit length in the backward direction along the edge of the strip; as a result the particle will ultimately move one step further along the same strip in the zig-zag direction in which it was moving forward at time $t + 3$. Therefore any trajectory eventually forms a zig-zag of length 4, leading to propagation in the direction of the zig-zag path. One can verify that after the turning back of the particle, the trajectory forms a parallelogram (Fig.12c).

Now the path of the particle through this parallelogram ends with three steps with velocity vectors: $\mathbf{C}((t+7)+)$, $\mathbf{C}((t+8)+)$, $\mathbf{C}((t+9)+)$ that together form a zig-zag pattern of length 3 (see caption of Fig. 12). But these three velocity vectors form together with $\mathbf{C}((t+10)+)$ a new zig-zag of length 4, i.e. a new blocking pattern (such as in Fig.12a), shifted one lattice unit length in the direction of propagation, with respect to the initial blocking pattern. The cases shown in the figures used for the demonstration are typical and all other cases are easily inferred from these typical situations, as the reader can verify. Consequently, we have shown that a blocking pattern always gets shifted by one lattice unit length along an edge of the strip in the direction of propagation, either after two time steps if the previous zig-zag motion is continued (Fig.11a), or after seven time steps if the trajectory is turned back and a parallelogram of motion is formed (Fig.12c).

Thus, the particle will always propagate along a strip in the direction determined by the blocking mechanism in this strip. For an (arbitrary) given initial velocity of the particle, propagation can only take place in one of four strips: two with angles $\pm\pi/3$ (strips F and U) and two with angles $\pm\pi$ (strips D_1 and D_2) with respect to the initial velocity direction. The ratios of the occurrence of propagation along the four strips can be evaluated from Fig.10 by examining all possible paths leading to a strip (see examples in Fig.11) and by giving weights q and $(1-q)$, to an R and an L scatterer, respectively. For $q = \frac{1}{2}$, these ratios are 3:3:1:1 for the directions F, U, D_1 and D_2 respectively.

Corollaries follow from Theorem 2.

Corollary 1 : The shortest time to create a blocking pattern is four time steps, and the longest time is ten time steps.

Proof : The proof follows straightforwardly by inspection of Figs.12a and 12c, where the zig-zag pattern of four velocities arranged in a W shape forms after 4 and 10 successive displacements of the particle, respectively (as verified by counting the number of arrows after the initial state).

Corollary 2 : The maximum number of visits to any site visited by the particle on the triangular lattice is six, and the maximum number of passages along any link connecting two neighboring sites is five.

Proof : Fig.12c. shows the longest trajectory executed by the particle to move one unit length along the lattice in the propagation strip. When the

scatterer configuration is such that the particle is again forced into a turn back motion (as in Fig.12b), when visiting the next site on the strip, the parallelogram of Fig.12c repeats itself (shifted upside down by one lattice unit length in the propagation direction). Then the middle site of the parallelogram, which has been visited three times (site ⑥ in Fig.12c) is visited three more times, yielding a total number of six visits. The number of visits to a site is then easily evaluated by counting the number of incoming arrows pointing to the site. For instance, in Fig.12c, there are three incoming arrows to site ⑥, and, when at the next time step, the particle undergoes backward motion thereby producing again the parallelogram trajectory (shifted upside down to the right), the three arrows pointing towards site ③ are now pointing to site ⑥, which yields a total number of six visits to site ⑥. This is the maximum number of visits since the blocking mechanism prevents the particle from ever coming back to this site. Similarly the number of passages along a link between two neighboring sites is evaluated by counting the number of arrows on that link. In the above example, which shows the typical case where the particle undergoes the longest possible trajectory to proceed in the propagation strip, the number of passages along link ③-⑥ is $3+2 = 5$.

Corollary 3: All visited sites located on one edge of the propagation strip are in the same state (R or L), and all sites located on the other edge are in the opposite state (L or R, respectively).

Proof: The blocking mechanism produces a zig-zag pattern with alternating velocity vectors (see Figs.11 and 12); as a result the states of the visited sites must be alternately R and L, or L and R. Consequently, the propagation dynamics triggers a reorganization of the states of the scatterers of the visited sites.

4.3 Statistical properties

We characterize the propagation process by the increase in the value of the coordinate of the particle along one edge of the propagation strip, as illustrated in Fig.13. We consider the situation where the particle visits site r for the first time, and we analyze how the particle proceeds from site r to the (next) site with coordinate $r + 1$ on the same side of the strip. Obviously, before arriving at site $r + 1$, the particle must go through a site with coordinate $r' = r + \frac{1}{2}$ on the other side of the strip (see Fig.13). At both site r

and site $r + \frac{1}{2}$, one of two possibilities occurs: either the particle trajectory continues a forward zig-zag path or it turns back. Thus, the transition from r to $r + 1$ can take place in four possible ways:

(*ff*) the particle continues a forward zig-zag path at both sites r and $r + \frac{1}{2}$;

(*fb*) the particle continues a zig-zag path at r and turns back at $r + \frac{1}{2}$;

(*bf*) the particle turns back at r , and goes into a forward zig-zag path at $r + \frac{1}{2}$;

(*bb*) the particle turns back both at r and at $r + \frac{1}{2}$.

So, in case (*ff*) the transition from r to $r + 1$ occurs in two forward time steps (see Fig.12a), and obviously takes longer in the other cases. Indeed, in section 4.2, we showed that if the particle turns back (see Fig.12b), it takes seven (6+1) time steps before it performs a zig-zag path again along the propagation strip (see Fig.12c). Therefore, the transition takes eight times steps in case (*fb*) – (1+7) corresponding to one step forward and one back turn – and (7+1) time steps in case (*bf*), while fourteen time steps are necessary in case (*bb*) – (7+7) corresponding to two back turns. It is easy to verify that the occurrence probabilities of the various cases are: $q(1 - q)$ for case (*ff*), q^2 for case (*fb*), $(1 - q)^2$ for case (*bf*), and $(1 - q)q$ for case (*bb*).

From the above results, we can write the equation for the first visit probability at site $r + 1$ at time t as

$$\begin{aligned} P_1(r + 1, t) &= [q^2 + (1 - q)^2]P_1(r, t - 8) \\ &+ q(1 - q)[P_1(r, t - 2) + P_1(r, t - 14)]. \end{aligned} \quad (4.1)$$

It follows from this expression that the average time it takes the particle to propagate one lattice unit length along a side of a strip is $\langle t \rangle = 8 [q^2 + (1 - q)^2] + 16 q(1 - q) = 8$ time steps, so that the average propagation velocity reads

$$\langle c \rangle = \frac{1}{\langle t \rangle} = \frac{1}{8}, \quad (4.2)$$

(in lattice unit lengths per time step), independently of q and of the direction of propagation.

When the particle is propagating in a strip, it takes an even number of time-steps to move from one site to the next on the edge of the strip in the forward direction (e.g. from r to $r + 1$ via r' in Fig.13) because of the blocking zig-zag pattern.¹⁰ Therefore when the particle arrives *for the first time* at

¹⁰A backward displacement (in the direction opposite to the propagation direction) can

site $r + 1$ (see Fig.13), site r cannot have been visited more than four times (as can be checked with Fig.12); so we can also write Eq.(4.1) as

$$P_1(r + 1, t) = q(1 - q)P_1(r, t - 2) + \sum_{\alpha=2}^4 P_\alpha(r, t - 2), \quad (4.3)$$

where, as can be verified using Fig.13 to explore all possible paths,

$$\begin{aligned} P_2(r, t - 2) &= (1 - q)^2 P_1(r, t - 8), \\ P_3(r, t - 2) &= q^2 P_1(r, t - 8), \\ P_4(r, t - 2) &= (1 - q)q P_1(r, t - 14). \end{aligned} \quad (4.4)$$

Now we define the total probability $P(r, t) = \sum_{\alpha=1}^4 P_\alpha(r, t)$, which, with (4.4), is given by

$$P(r, t) = P_1(r, t) + [q^2 + (1 - q)^2]P_1(r, t - 6) + q(1 - q)P_1(r, t - 12). \quad (4.5)$$

In (4.5), we use equation (4.1) for $P_1(r, t')$ with $t' = t, t - 6, t - 12$, and in the result, we combine the various terms to obtain a closed equation for the total probability

$$\begin{aligned} P(r, t) &= q(1 - q)[P(r - 1, t - 2) + P(r - 1, t - 14)] \quad (4.6) \\ &\quad + [q^2 + (1 - q)^2]P(r - 1, t - 8). \quad (4.6) \end{aligned}$$

We observe that $P(r, t)$ obeys the same equation as $P_1(r, t)$, Eq.(4.1), and it can be shown [7] that its continuous limit has the same structure as Eq.(3.43).

4.4 Long-time behavior

To investigate the long-time behavior of the particle motion, we proceed along the same lines as in the one-dimensional case. We start with the Laplace-Fourier transformation of Eq.(4.1), which yields

$$e^{vk} \left[e^{14s} \tilde{f}_k(s) - \sum_{m=1}^7 e^{2m} s f_k(t = 14 - 2m) \right] =$$

only take place along the edge of the strip and takes one time step since, because of the blocking mechanism, it cannot exceed one lattice unit length.

$$\begin{aligned} & \left[q^2 + (1 - q)^2 \right] \left[e^{6s} \tilde{f}_k(s) - \sum_{m=1}^3 e^{2m} s f_k(t = 6 - 2m) \right] + \\ & q(1 - q) \left[(1 + e^{12s}) \tilde{f}_k(s) - \sum_{m=1}^6 e^{2m} s f_k(t = 12 - 2m) \right], \end{aligned} \quad (4.7)$$

where $f_k(t)$ denotes the space-Fourier transform of $P_1(r, t)$, and $\tilde{f}_k(s)$ its Laplace transform. In the limit $k = 0$, we obtain

$$\tilde{f}_{k=0}(s) = \frac{h(s)}{g(s)} \quad (4.8)$$

with

$$\begin{aligned} h(s) = & \left[\sum_{m=1}^7 e^{2ms} f_{k=0}(14 - 2m) \right] - q(1 - q) \left[\sum_{m=1}^6 e^{2ms} f_{k=0}(12 - 2m) \right] \\ & - [q^2 + (1 - q)^2] \left[\sum_{m=1}^3 e^{2ms} f_{k=0}(6 - 2m) \right], \end{aligned} \quad (4.9)$$

and

$$g(s) = e^{14s} - q(1 - q)e^{12s} - [q^2 + (1 - q)^2]e^{6s} - q(1 - q). \quad (4.10)$$

To solve Eq.(4.8), we need to know the ‘‘initial conditions’’, i.e. the values of $f_k(t)$ at $t = 2m$, for $m = 0, \dots, 6$. The values of $f(r, t)$ at $t = 0, \dots, 12$ are obtained from the particle dynamics discussed in the previous section and are given in Appendix B, along with their corresponding Fourier transforms. We insert these values in (4.9), and, since we are interested in the long-time behavior, we consider the limit $\tilde{f}_{k=0}(s \rightarrow 0)$ by expanding $\tilde{f}_{k=0}(s)$ to lowest significant order in s ; the result is

$$\lim_{s \rightarrow 0} \tilde{f}_{k=0}(s) = \frac{1}{8s}, \quad (4.11)$$

which, by inverse transformation, yields

$$\lim_{t \rightarrow \infty} f_{k=0}(t) = \frac{1}{8} = \langle c \rangle. \quad (4.12)$$

Thus, as for the one-dimensional case, we find that in the long-time limit, $f_{k=0}(t \rightarrow \infty) \equiv \lim_{t \rightarrow \infty} \sum_r P_1(r, t)$ is equal to the average propagation velocity, with the difference that, in the triangular lattice, $\langle c \rangle$ is independent

of q . Furthermore it can be shown [7] that the long-time solution of Eq.(4.1) is given by

$$P_1(r, t)|_{t \gg 1} = \sqrt{\frac{2}{\pi}} \frac{1}{(\tilde{\gamma}r)^{1/2}} \exp -\frac{(t - \langle t \rangle)^2}{2\tilde{\gamma}r}, \quad (4.13)$$

with $\langle t \rangle = r/\langle c \rangle = 8r$ and $\tilde{\gamma} = 72pq$. In Fig.14 we present numerical simulations and show that our theoretical result (4.13) is in agreement with the simulation data.

5 Concluding comments

1. By replacing spins \uparrow and \downarrow by 1's and 0's respectively, the initial state of the 1-D spin lattice can be read as the input string of the tape of a Turing machine whose control device is the particle; the controller performs operations according to the rules of the flipping spins and writes the output on the tape as the final spin configuration also converted into 1's and 0's. Here the computation algorithm performs the binary addition of the initial string with itself followed by a "XOR" with 1 (which is equivalent to $1 \Leftrightarrow 0$ plus a shift). In the triangular lattice, one can similarly interpret the state of the scatterers along the edges of the propagation strip as R/L \rightarrow 0/1; then the algorithm performs the logical operations "AND" and "NAND" with 0 alternately on each side of the strip, which transforms a random sequence of 0's and 1's into a periodic string ...01010101... .

2. After the passage of the particle through the one-dimensional lattice, all the spins are in the state opposite to their initial state ($\uparrow \Leftrightarrow \downarrow$) with one lattice site shift in the direction opposite to the propagation direction. Consider that the system is made periodic (i.e. on a circle) by identifying the first and last sites of the chain, and that the particle propagates clockwise on the circle; then there is a counterclockwise drift (two lattice sites back) of the initial spin configuration every two cycles, and the average propagation velocity is given by $c(q) = \frac{1}{2}[\frac{1}{3-2q} + \frac{1}{3-2(1-q)}]$. Similarly, when, in the triangular lattice, one attaches the two beginning and two end sites of a strip crosswise, the particle undergoes periodic motion on the strip.

3. Propagation has also been observed in the square lattice fully occupied with flipping scatterers when the scatterers are distributed periodically over the lattice [2]. However, not in all such cases does propagation occur during the time span of the simulations ($\leq 10^7$ time steps). It remains therefore an open question whether propagation on the square lattice, periodically covered with flipping scatterers, always occurs or only for a certain class of periodic scatterer patterns. When it occurs, propagation seems always to take place in a strip (like on the triangular lattice), which shows similarity with the glider behavior in the Game of Life [10]. Although the precise blocking mechanism is not known for the square lattice, “immediate” propagation can occur, which would imply then the possibility of an “instantaneous” blocking on the square lattice.

4. Propagation on the one-dimensional and triangular lattices occurs for scattering angles of $\pm\pi$ and $\pm 2\pi/3$, respectively. For those cases on the periodically occupied square lattice where propagation has been found, the scattering angle equals $\pm\pi/2$, while for the randomly occupied square lattice, the maximum angle scattering rule yields a(n) (average) value larger than $\pi/2$. On the other hand, a scattering angle of $\pm\pi/3$ on the triangular lattice leads to the motion of the particle on a honeycomb (hexagonal) lattice where no propagation seems to occur for flipping scatterers [2]. One might therefore conjecture that propagation only occurs in lattices fully occupied with flipping scatterers, when the scattering angle is $\geq \pi/2$ in absolute value.

5. Notice that in the development performed for the triangular lattice, we have not used the regularity property of the Bravais lattice. So the results should not be dependent of this property and should also be valid for the random triangular lattice such as the Delaunay lattice (see Fig.1), provided the scattering rule is set such that the particle is deflected with the largest possible angle ($> \pi/2$). However, because of the topological randomness of the Delaunay lattice, one cannot predict whether the trajectory of the particle will remain unbounded.

6. To the best of our knowledge, it is an open question whether particle dynamics in three dimensional lattices with flipping scatterers can exhibit propagation or other peculiar behaviors.

Appendix A

Here we derive the expression for the propagation velocity of a particle moving in a 1-D lattice with flipping spins, directly from the particle dynamics described in section 2.2. The average asymptotic propagation velocity is given by

$$\langle c \rangle = \lim_{t \gg \Delta t} C(t), \quad (\text{A.1})$$

with

$$C(t) = \frac{R(t) - R(0)}{t}, \quad (\text{A.2})$$

and where Δt is the unit time step ($\Delta t = 1$, i.e. the limit in (A.1) will be taken as $t \rightarrow \infty$). It follows by iteration from Eq.(2.1), that

$$R(t) - R(0) = C(t-1) + C(t-2) + \dots + C(0) = \sum_{\tau=0}^{t-1} C(\tau). \quad (\text{A.3})$$

When we consider the velocity of the particle at two successive time-steps, five cases must be examined as described in Table 1 (see also Fig.15). If the particle arrives at a site at time $\tau-1$ with velocity $C(\tau-1)$ and leaves the site with velocity $C(\tau)$, we observe that when taking the sum over the velocities, all $C(\tau-1)$'s and $C(\tau)$'s which do not cancel are those which correspond to particle displacements leading to a site visited by the particle for the first time. So the sum $\sum_{\tau} C(\tau)$ is equal to the number N_f of displacements which, during time t , lead to a *first visit*. Now, since the particle undergoes a displacement at each time-step, the total number of displacements N_t during time t , is equal to t . Consequently, from (A.1)-(A.3), we have

$$\langle c \rangle = \lim_{t \rightarrow \infty} \frac{1}{t} [R(t) - R(0)] = \lim_{t \rightarrow \infty} \frac{1}{t} \sum_{\tau=0}^{t-1} C(\tau) = \lim_{t \rightarrow \infty} \frac{N_f(t)}{N_t(t)}; \quad (\text{A.4})$$

and, since $N_f(t)/N_t(t)$ is just $\sum_r P_1(r, t)$, it follows that

$$\langle c \rangle = \lim_{t \rightarrow \infty} \sum_r P_1(r, t) = \lim_{t \rightarrow \infty} f_{k=0}(t) = \frac{1}{3-2q} \equiv c(q), \quad (\text{A.5})$$

where we have used (3.16).

TABLE 1				
Fig. 15	The particle arrives at site r for the	with velocity $C(\tau - 1)$	and leaves site r with velocity $C(\tau)$	The next site is visited for the
(a)	first time	$C = +1$	$C = +1$	first time
(b)	first time	$C = +1$	$C = -1$	second time
(c)	second time	$C = +1$	$C = +1$	first time
(d)	second time	$C = -1$	$C = +1$	second time
(e)	third time	$C = -1$	$C = +1$	second time

Appendix B

The “initial conditions” for the computation of the long-time behavior of the function $f_{k=0}(t) \equiv \sum_r P_1(r, t)$ in section 4.4, are given by the following expressions

$$\begin{aligned}
f(r, t = 0) &= \delta_{r,0}, \\
f(r, t = 2) &= q(1 - q) \delta_{r,1}, \\
f(r, t = 4) &= q^2(1 - q)^2 \delta_{r,2}, \\
f(r, t = 6) &= q^3(1 - q)^3 \delta_{r,3}, \\
f(r, t = 8) &= q^4(1 - q)^4 \delta_{r,4} + [q^2 + (1 - q)^2] \delta_{r,1}, \\
f(r, t = 10) &= q^5(1 - q)^5 \delta_{r,5} + 2q(1 - q)[q^2 + (1 - q)^2] \delta_{r,2}, \\
f(r, t = 12) &= q^6(1 - q)^6 \delta_{r,6} + 3q^2(1 - q)^2[q^2 + (1 - q)^2] \delta_{r,3}, \quad (\text{B.1})
\end{aligned}$$

and correspondingly, in Fourier transform, by

$$\begin{aligned}
f_k(0) &= 1, \\
f_k(2) &= q(1 - q) e^{ik}, \\
f_k(4) &= q^2(1 - q)^2 e^{2ik}, \\
f_k(6) &= q^3(1 - q)^3 e^{3ik}, \\
f_k(8) &= q^4(1 - q)^4 e^{4ik} + [q^2 + (1 - q)^2] e^{ik}, \\
f_k(10) &= q^5(1 - q)^5 e^{5ik} + 2q(1 - q)[q^2 + (1 - q)^2] e^{2ik}, \\
f_k(12) &= q^6(1 - q)^6 e^{6ik} + 3q^2(1 - q)^2[q^2 + (1 - q)^2] e^{3ik}. \quad (\text{B.2})
\end{aligned}$$

Acknowledgments

PG benefited from a stay at Rockefeller University whose hospitality is gratefully acknowledged. JPB acknowledges support by the *Fonds National de la Recherche Scientifique* (FNRS, Belgium). EGDC gratefully acknowledges support from the *Belgian Franqui Foundation* and the hospitality of the *Center for Nonlinear Phenomena and Complex Systems* at the Université Libre de Bruxelles, which made an extended stay in Brussels possible, during which a collaboration with PG and JPB initiated this work. EGDC also acknowledges support from the US Department of Energy under grant number DE-FG02-88-ER13847. LAB was partially supported by NSF grant number DMS-963063. EGDC and LAB thank the *Erwin Schrödinger Institute* (Vienna) for its hospitality and support.

References

- [1] C.G. Langton, *Physica D*, **22**, 120 (1986); D. Gale, *The Mathematical Intelligencer*, **15**, 54 (1993); S.E. Troubetskoy, *Lewis-Parker Lecture* (1997), and references therein.
- [2] X.P. Kong and E.G.D Cohen, *J. Stat. Phys.*, **62**, 737 (1991); E.G.D. Cohen and F. Wang, *J. Stat. Phys.*, **81**, 445 (1995); *ibid*, *Physica A*, **219**, 56 (1995), and references therein; H-F. Meng and E.G.D. Cohen, *Phys. Rev. E*, **50**, 2482 (1994).
- [3] L.A. Bunimovich and S.E. Troubetskoy, *J. Stat. Phys.*, **74**, 1 (1994), and references therein; L.A. Bunimovich, *Int. J. Bifur. & Chaos*, **6**, 1127 (1996).
- [4] See also F. Wang and E.G.D. Cohen, *J. Stat. Phys.*, **84**, 233 (1996).
- [5] See also Eq.(14) in E. G. D. Cohen, “New types of diffusion in lattice gas cellular automata” in *Microscopic Simulations of Complex Hydrodynamic Phenomena*, M. Mareschal and B. L. Holian, eds., NATO ASI Series B: Physics Vol. 292, p.145.
- [6] See e.g. W. Feller, *An Introduction to Probability Theory* (Wiley, New York, 3d ed., 1968), Vol.1, section XIV.6.
- [7] The continuous limit of Eq.(3.3) and the comparison with the continuous limit of the BRW equation are discussed in a paper by J.P. Boon (to be published).
- [8] Reference [6], section XI.2; see also N. Van Kampen, *Stochastic Processes* (North Holland, Amsterdam, 1990), section IV.6.
- [9] Reference [6], section VII.2.
- [10] H. A. Peelle, “The Game of Life” in: *Recreational Computing*, Vol. 7 (1979), pp. 16-27; E. Berlekamp, J. Conway, and R. Guy, “What is Life” in: *Winning Ways*, Vol 2, (Academic Press, 1982), ch.25.

Figure captions

Fig. 1. Propagation in a random Delaunay lattice, where the particle arriving at a site of the random lattice is deflected over the largest possible angle there, either to the right or to the left, depending on the R or L nature of the scatterer. Arrows illustrate particle displacements. The shaded area shows the propagation strip.

Fig. 2. Scattering on the one-dimensional lattice illustrating the proof of *Theorem 1* (see text); the blocking patterns are framed with dotted squares.

Fig. 3. Example of spin reorganization in 1-D lattice. The broken line is the particle trajectory. Black dots are sites with spin down, and open squares (shown only for the initial and final configurations) are sites with spin up. The spin reorganization is well observed by comparing the top row with the bottom row: $\bullet \Leftrightarrow \square$ (with one site shift to the left).

Fig. 4. Propagation velocity in 1-D lattice: for $q = 1$ (all spins initially up) $\langle c \rangle = 1$ (upper line); $q = 0.5$ (for two different spin configurations; middle lines) $\langle c \rangle = 1/2$; and $q = 0$ (all spins initially down) $\langle c \rangle = 1/3$ (lower line).

Fig. 5. $f_{k=0}(t)$ as a function of t for $q = 0.1$. Simulation results (dots) and theory, Eq.(3.13) (lines).

Fig. 6. Space-time evolution of $P_1(r, t)$ for $q = 0.5$. The x-axis denotes space.

Fig. 7. The probability $P_1(r, t)$ as a function of r at $t = 500$. Simulation data (black dots), binomial expression (3.23) (open circles), and Eq.(3.29) (curve).

Fig. 8. Situations on the 1-D lattice leading to second visits, (a) and (b), and to third visit, (c).

Fig. 9. Typical example of propagation pattern in triangular lattice. The initial position of the particle is shown by a full diamond; the propagation direction is along the upper left axis of the lattice. The coordinates are marked in lattice unit lengths.

Fig. 10. Propagation strips on the triangular lattice. The initial velocity of the particle, $\mathbf{C}(t_0)$, is shown as the heavy arrow. When the particle arrives at one of the sites marked \odot , it is trapped in one of the propagation strips bounded by parallel heavy solid lines. The four propagation directions are indicated by arrows and capital letters (F, U, D₁, D₂).

Fig. 11. Examples of trajectories leading to propagation in one of the four directions (F, U, D₁ or D₂). Light arrows indicate the successive velocity vectors of the particle after the initial state ($\mathbf{C}(t_0)$, heavy arrow).

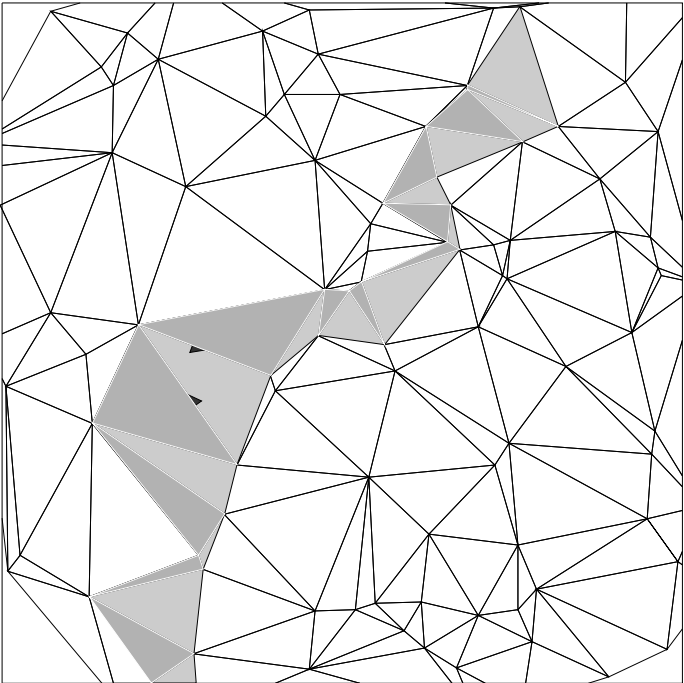
Fig. 12. Formation of blocking pattern by direct forward zig-zag path (a), and by turn back motion (b) followed by zig-zag trajectory emerging from parallelogram path (c). Light arrows indicate the successive velocity vectors of the particle. Vectors $\mathbf{C}((t+7)+)$, $\mathbf{C}((t+8)+)$, $\mathbf{C}((t+9)+)$, and $\mathbf{C}((t+10)+)$ are along the links $\textcircled{2}-\textcircled{3}$, $\textcircled{3}-\textcircled{6}$, $\textcircled{6}-\textcircled{*}$, and $\textcircled{*}-\textcircled{}$, respectively.

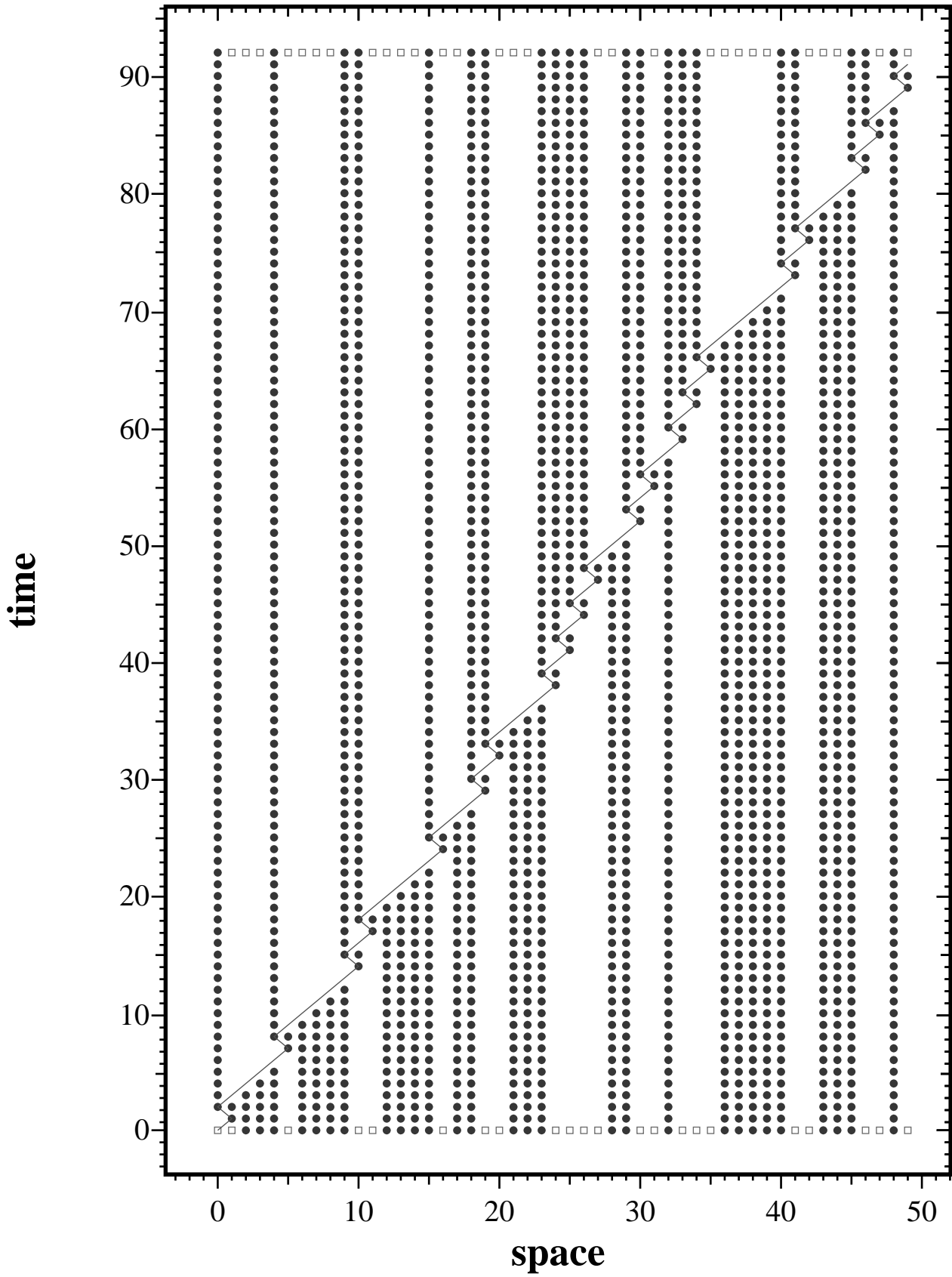
Fig. 13. Particle motion from site r to site $r+1$ along the propagation strip *via* site $r' = r + \frac{1}{2}$. The arrow pointing to the right shows the propagation direction.

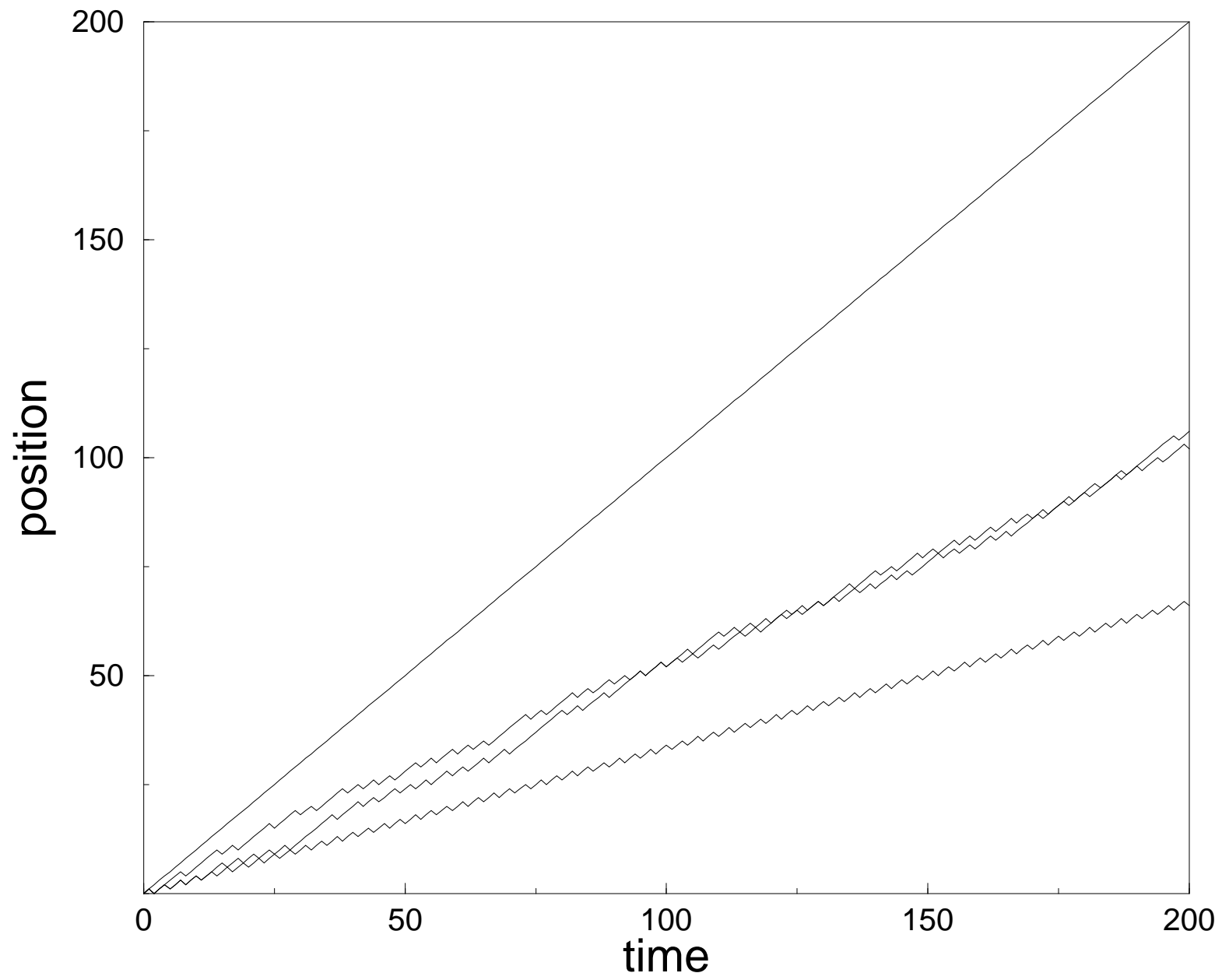
Fig. 14. Long-time behavior in triangular lattice. $P_1(r, t)$ as a function of r after 7616 time-steps: numerical data from simulation measure-

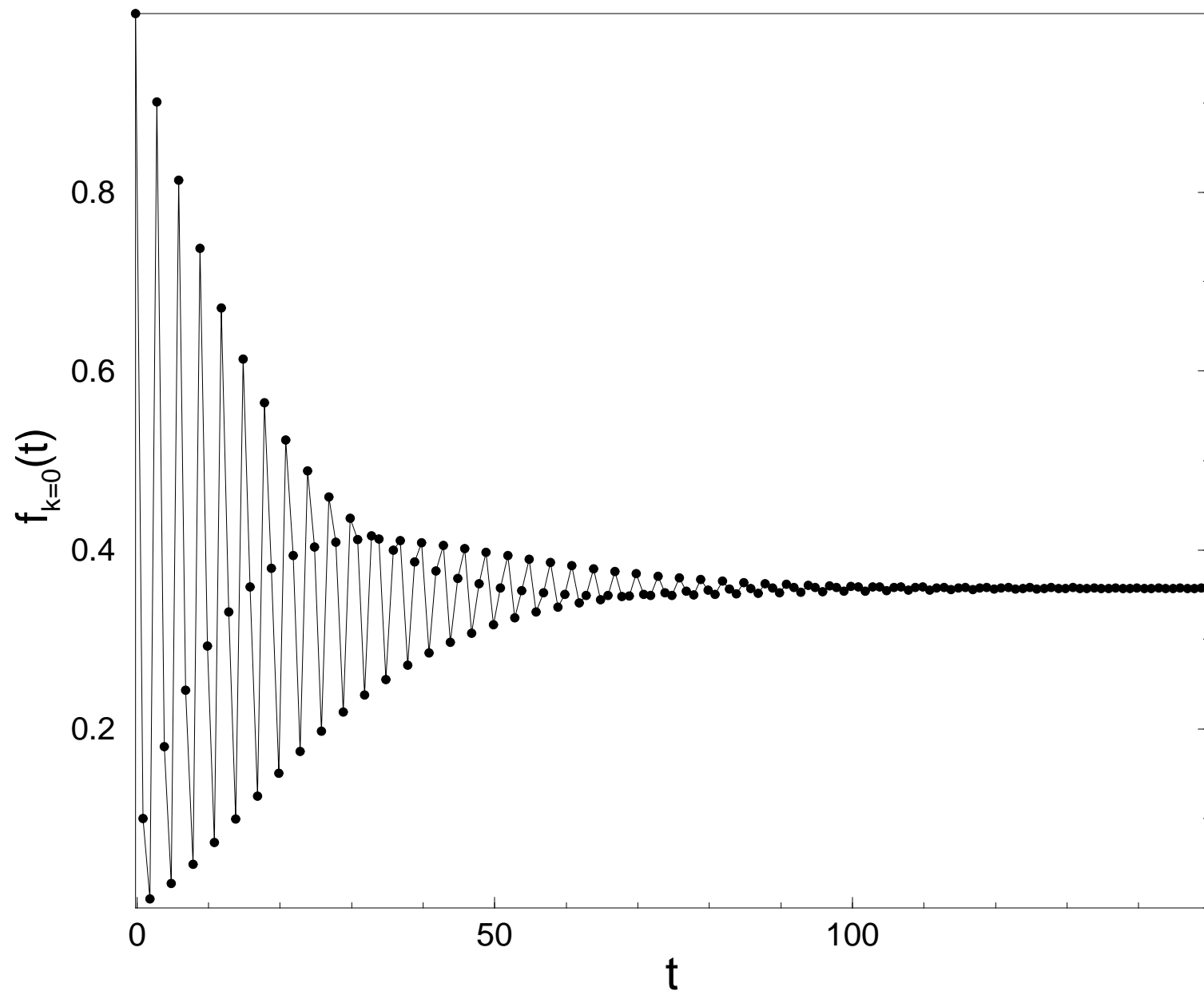
ments (black dots) compared with analytical result (4.13) (full curve).

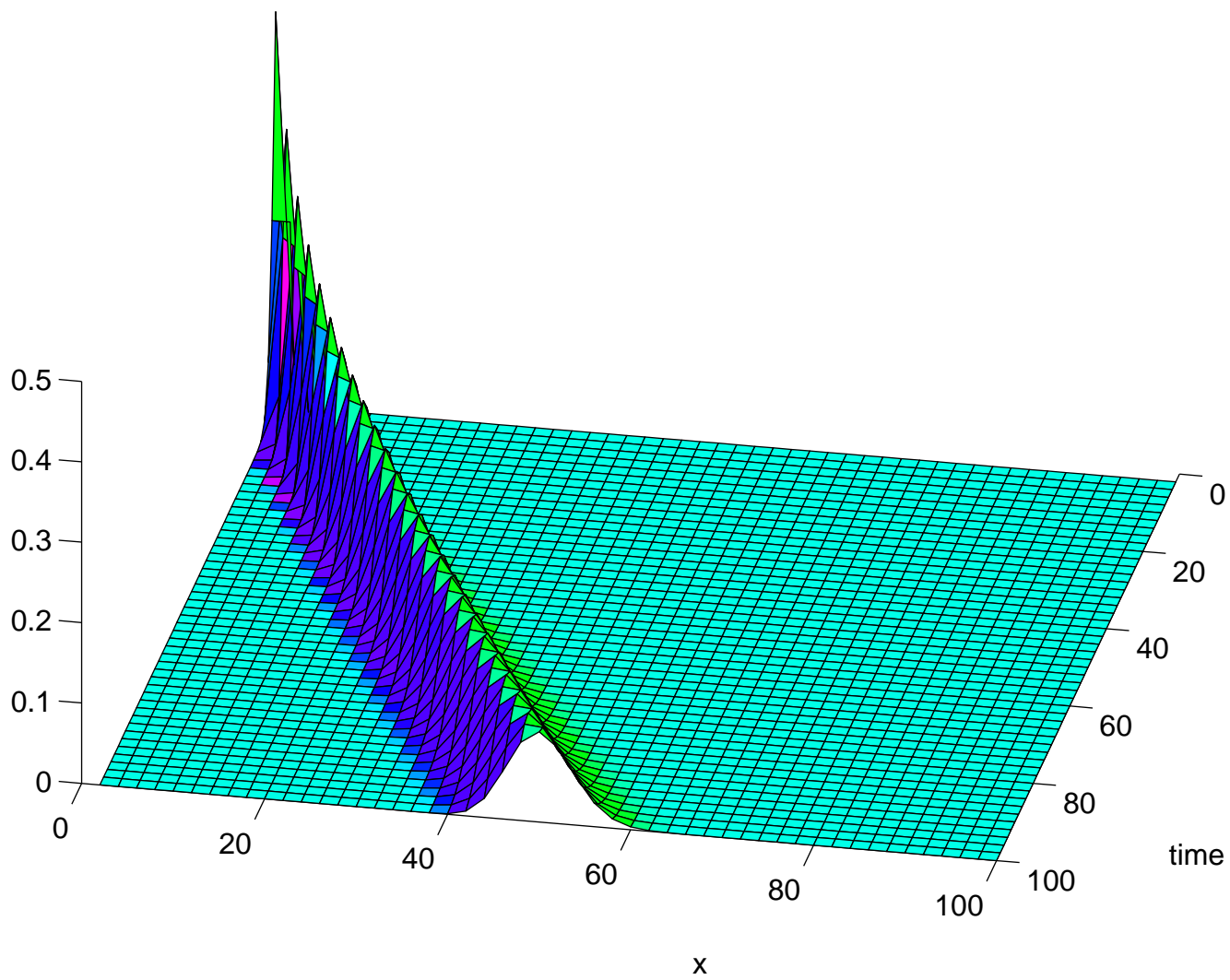
Fig. 15. Illustration of the five cases discussed in Appendix A and described in Table 1.

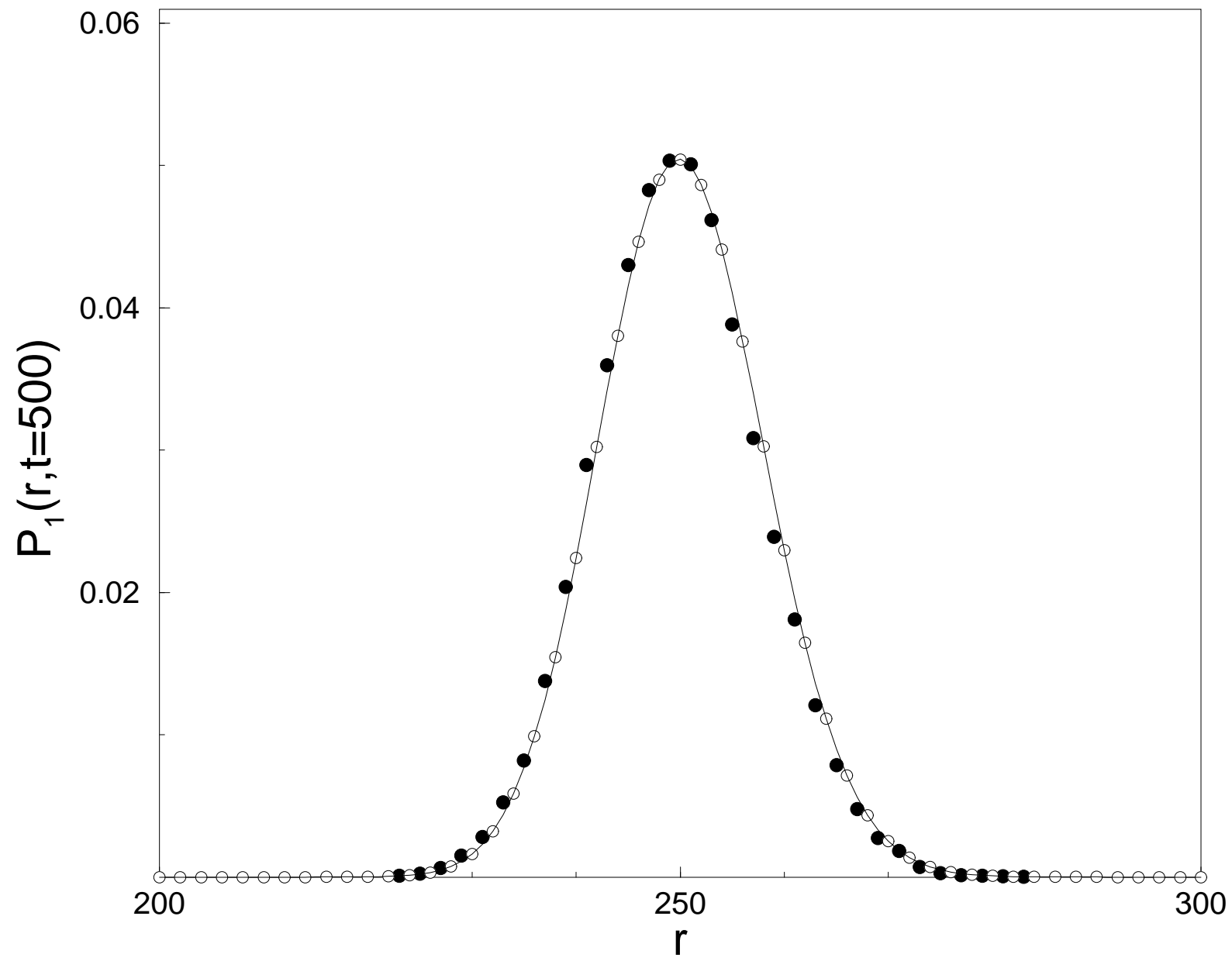


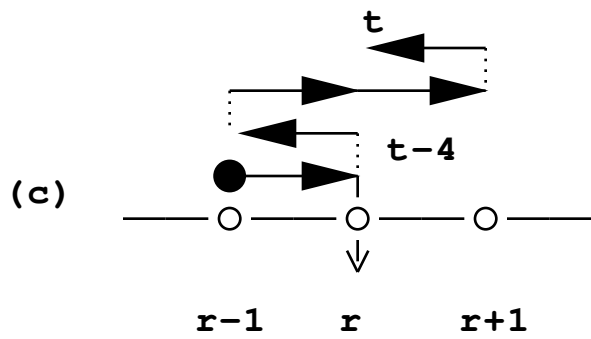
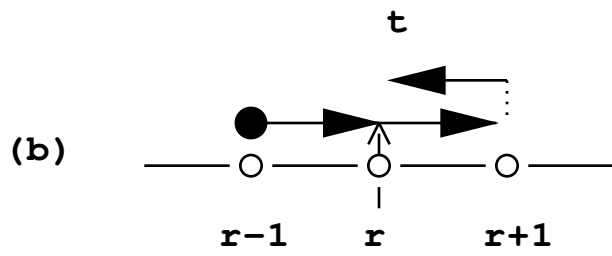
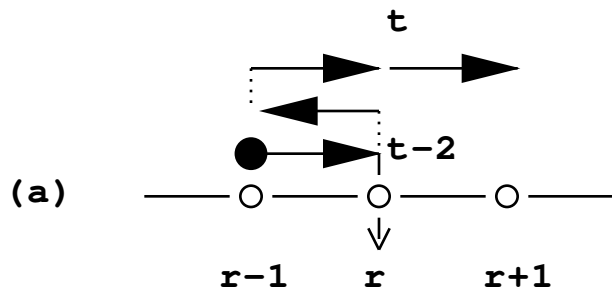


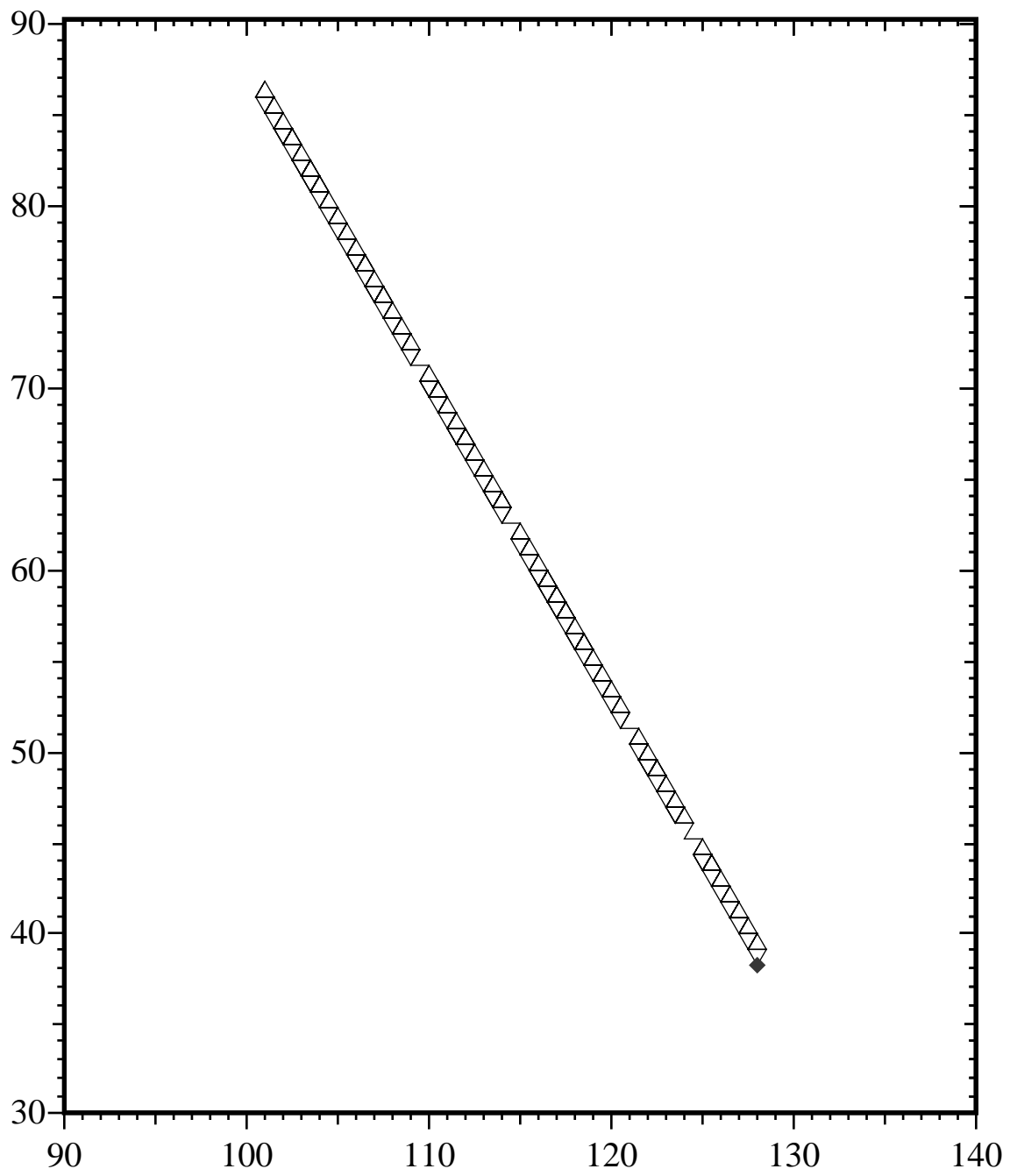


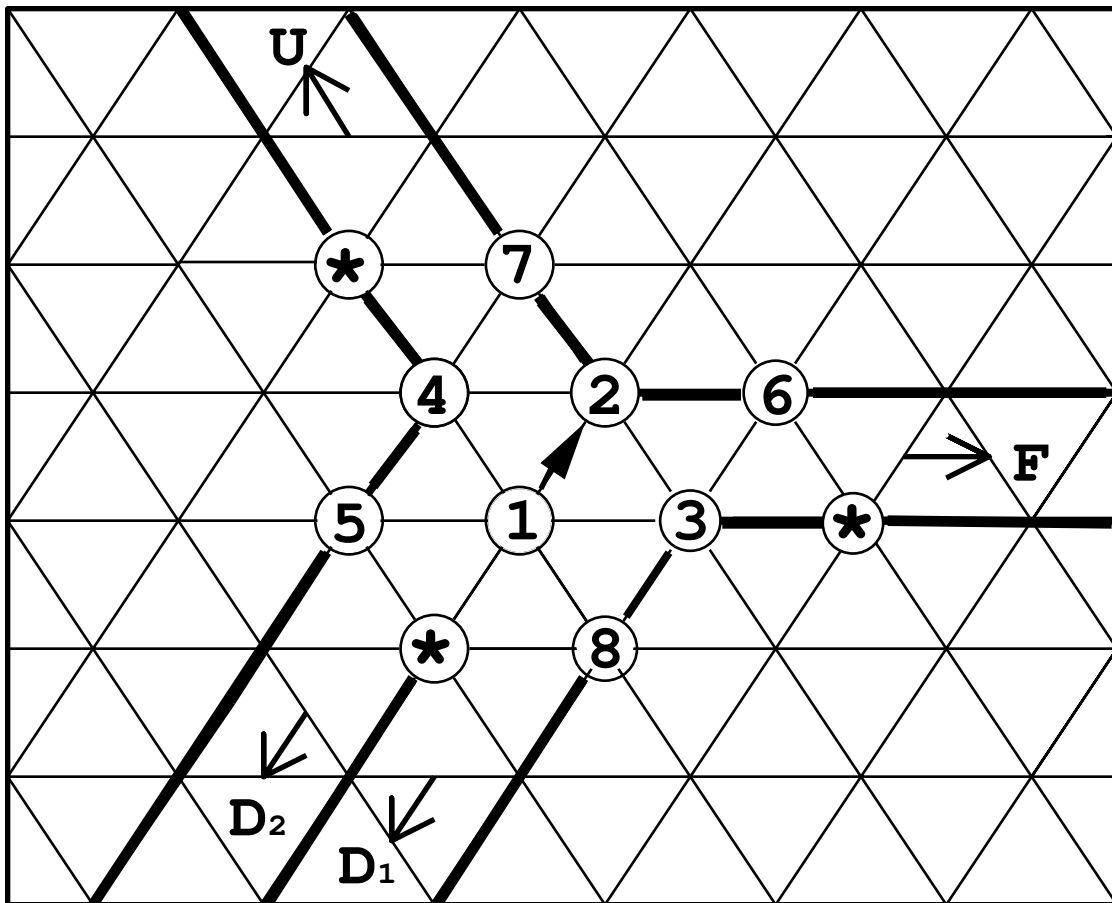




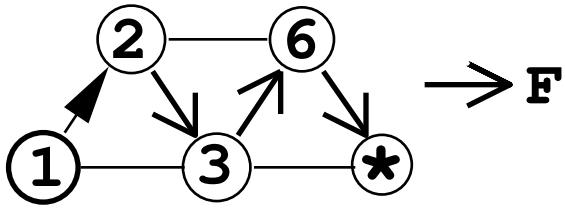




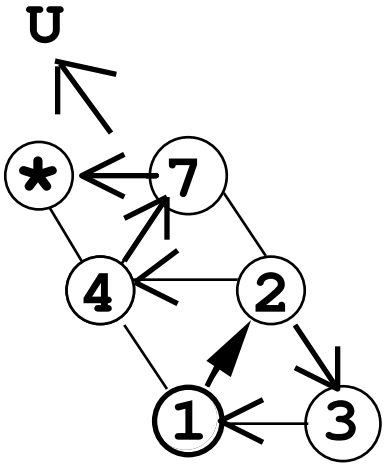




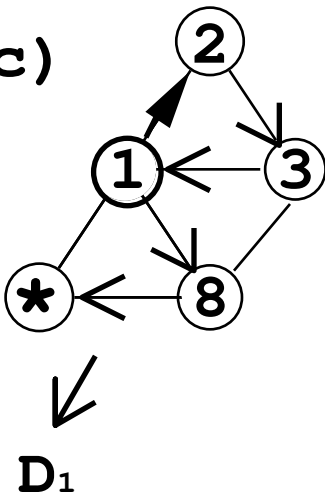
(a)



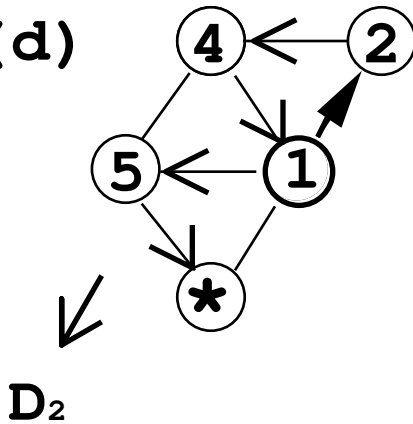
(b)



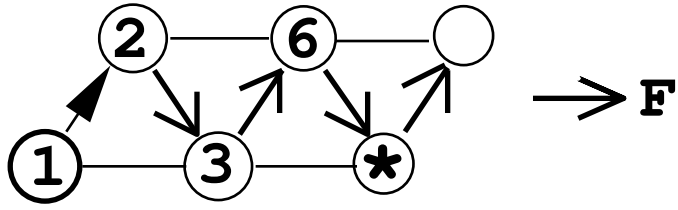
(c)



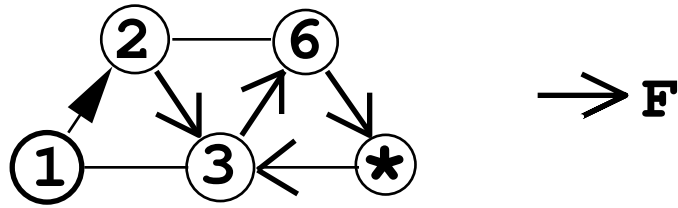
(d)



(a)



(b)



(c)

